Infrared Spectroscopic Investigation of CO Adsorption on SBA-15- and KIT-6-Supported Nickel Phosphide Hydrotreating Catalysts

Tamás I. Korányi,*,† Éva Pfeifer,† Judith Mihály,† and Karin Föttinger‡

Department of Molecular Spectroscopy, Institute of Structural Chemistry, Chemical Research Center of the Hungarian Academy of Sciences, P.O. Box 17, H-1525 Budapest, Hungary, and Institute of Materials Chemistry, Vienna University of Technology, Veterinärplatz 1, A-1210 Vienna, Austria

Received: December 20, 2007; Revised Manuscript Received: March 20, 2008

The infrared (IR) spectra of CO adsorbed on 10, 20, and 30 wt % nickel phosphide-containing reduced SBA-15 and KIT-6 mesoporous silica-supported catalysts have been studied at 300−473 K. On the catalysts containing a stoichiometric amount of phosphorus with 20 wt % loading, the most intense IR absorption band was observed at 2097−2099 cm^{-1}, which was assigned to CO terminally bonded to coordinatively unsaturated Ni$^{\delta+}$ ($0 < \delta < 1$) sites. The frequency of this band was 15 cm^{-1}, higher than that in the spectrum of a reduced Ni_2P/SiO_2 catalyst, indicating a modified Ni−P charge distribution. This band shifted to lower wavenumbers, and its intensity decreased, while the relative intensity of another band at 2191−2194 cm^{-1} assigned to CO terminally bonded to P increased going to catalytically less active, excess-P-containing SBA-15-supported catalysts. CO also adsorbed as a bridged carbonyl (1910 cm^{-1}) and as $Ni(CO)_4$ (2050 cm^{-1}) species, and the formation of surface carbonates was also identified. The nature of the surface acidity was studied by temperature-programmed desorption of ammonia (NH_3-TPD). Weak and strong acid sites were revealed, and the high excess-P-containing catalyst released the highest amount of ammonia, indicating that a high concentration of strong acidity can be disadvantageous for reaching high hydrotreating catalytic activity. The modified Ni−P charge distribution, the mode of CO adsorption on surface nickel phosphide sites, as well as the acidity can be directly connected to the catalytic activity of these mesoporous silica-supported catalysts.

Introduction

The more stringent fuel specifications (ultraclean transformation fuels) demand a search for new efficient hydrotreating catalysts. Hydrotreating refers to a series of refinery processes aiming at the production of clean motor fuels by removing sulfur (hydrodesulfurization, HDS), nitrogen (hydrodenitrogenation, HDN), and metals from the organic matter in oil feedstock.[1] Silica-supported transition-metal phosphides outperform the traditional Co(Ni)−Mo/Al_2O_3 hydrotreating catalysts in model catalytic studies.[2] However, the application of new high-surface-area catalyst supports is required to gain better metal phosphide catalysts.

Recently, a large variety of new carbon-[3,4] and mesoporous silica-based carriers, such as MCM-41,[5] HMS,[6] and so forth, have been studied for hydrotreating catalysts. We have reported the characterization of CMK-5[7] carbon- and SBA-15[7,8] mesoporous silica-supported nickel phosphide hydrotreating catalysts. SBA-15 is a mesoporous silica composed of two-dimensional hexagonal arrays of uniformly sized channels with diameters in the range of 5−9 nm.[9] The turnover rates of SBA-15-supported catalysts were much higher than the relevant rates of Ni_2P/SiO_2 catalysts.[8]

Infrared (IR) spectroscopy of adsorbed probe molecules (CO, NO, NH_3, and pyridine) on catalytic surfaces is widely applied for the determination of concentration, nature, and acidity of catalytic active sites.[10] CO is a typically chosen probe molecule since it is generally unreactive and its small molecular size enables it to probe all available catalytic sites. CO is often used to estimate active site densities of catalysts. Its C−O stretching frequency is well characterized for CO adsorption on most metal surfaces.[11,12] The surface chemistry of CO on reduced and sulfided Ni_2P/SiO_2 catalysts has been investigated with IR spectroscopy.[13,14] Either four[13] or three[14] different ν_{CO} absorption bands were observed, indicating various adsorbed species on the surface of reduced and sulfided Ni_2P/SiO_2 catalysts (Table 1).

This letter reports on the infrared spectroscopic investigation of CO adsorption on SBA-15- and KIT-6-supported nickel phosphide catalysts. The structure of KIT-6 may be described by the gyroid infinite periodic minimal surface (IPMS) structure with cubic *Ia*3*d* symmetry, being structurally similar to smaller-pore MCM-48 silica.[15] In addition to IR investigations, the nature of surface acidity was studied by temperature-programmed desorption of ammonia (NH_3-TPD). Our objective in this research is to extend the IR and NH_3-TPD studies from Ni_2P/SiO_2 to these catalysts from room temperature up to higher (473 K) temperatures in order to obtain information about the effect of active phase dispersion, acidity, and surface CO coverage on the mode of CO adsorption over SBA-15- and KIT-6-supported nickel phosphide catalysts.

Experimental Section

Catalyst Preparation. Five and two catalyst precursors were prepared by incipient wetness impregnation of SBA-15 and KIT-6 supports, respectively. Solutions with desired stoichiometric amounts of Ni as $Ni(NO_3)_2$ and P as $(NH_4)H_2PO_4$ were

---

* To whom correspondence should be addressed. Tel: +3614381100. Fax: +3614381143. E-mail: koranyi@chemres.hu.

† Chemical Research Center of the Hungarian Academy of Sciences.

‡ Vienna University of Technology.

10.1021/jp711935n CCC: $40.75

TABLE 1: CO Stretching Frequencies of Different Adsorbed Species on Reduced Catalyst Samples and Literature Reference[13,14] Values on Reduced and Sulfided Ni_2P/SiO_2 Catalysts

ν_{CO} absorbances	SBA20	SBA_E	SBA_H	KIT20	SBA10	SiO_2[13]	SiO_2[14]
$P{=}C{=}O$[a]	2191w	2194m	2191m	2193w	2185m	2196w	
$Ni^{\delta+}{-}CO$[a]	2099vs	2093s	2085m	2097vs	2083m	2083vs 2093vs[g]	2082vs
$Ni(CO)_4$[a]	2050sh				2050sh	2056sh	2056sh
$Ni^{\delta+}_2 > CO$ bridge[a]	1910w	1910w	1910vw	1912w	1903w	1914w	1912w
surface CO_3^{2-}[a]	1622vw 1406w	1613vw 1395vw	1615m 1410vw		1612m 1406w		
$P{=}C{=}O$[b]	2186vvw	2194m	2187m	2195m	2185m		
$Ni^{\delta+}{-}CO$[b]	2085s	2083m	2085m	2095s	2088m		
surface CO_3^{2-}[b]	1627m 1406m	1613m 1395vvw	1618s 1402vvw	1554m 1408m	1612s 1406m		
$Ni^{\delta+}{-}CO$[c]	2082m[e]	2070w[e]	2070w[d]	2088m[f]	2059w[d]		
surface CO_3^{2-}[c]	1622m[d] 1406w[d]	1613s[e] 1395vvw[e]	1618s[e] 1401w[e]	1550m[f] 1408m[e]	1612m[d] 1406w[d]		

[a] For 5 mbar of CO adsorbed for 10 min. [b] For 5 mbar of CO adsorbed for 30 min. [c] Following evacuation of 5 mbar of CO. [d] Following evacuation at 300 K only. [e] Following evacuation up to 373 K. [f] Following evacuation up to 423 K. [g] Sulfided Ni_2P/SiO_2 catalyst.

impregnated in SBA-15 or KIT-6 to arrive at Ni_2P loadings of 10 (SBA10), 20 (SBA20, KIT20), and 30 (SBA30, KIT30) wt %, followed by drying at 393 K. In addition, precursors for Ni as nickel phosphide with the SBA20 composition were prepared by initial P/Ni = 2 (high excess phosphorus, denoted by subscript H as SBA_H) and P/Ni = 0.8 (excess P, denoted by subscript E as SBA_E) ratios. The dried catalyst precursors were reduced in a hydrogen flow at 873 K, and following the cooling down to room temperature, the catalysts were passivated in a flow of 1 vol % O_2 in N_2. Further details of the catalyst preparation procedure and physicochemical data of the catalysts are given in ref 8.

Infrared Spectroscopic Investigation of CO Adsorption. The infrared spectra of adsorbed CO were recorded on a Bruker IFS 28 FT-IR spectrometer equipped with an MCT (mercury−cadmium−telluride) detector (resolution of 4 cm^{-1}, accumulation of 256 spectra). The 50−100 mg samples were prepared as self-supporting wafers (2 cm diameter), placed inside of an in situ adsorption cell, which allowed evacuation, static treatment in CO, and heating of the samples up to 573 K. Since the activation procedure was very important, different evacuation, reduction, and CO treatment conditions were used. The reduction in H_2 and then the CO adsorption were carried out under static conditions following evacuation to 10^{-5} mbar. Spectra of the best quality were obtained when the next activation and CO treatment procedure were followed: first, the sample was reduced in 500 Torr of hydrogen at 573 K for 30 min, then evacuated at 573 K for 30 min, and then reduced again in 500 Torr of hydrogen at 573 K for 30 min. In the fourth step, the sample was cooled to 300 K during a second evacuation when the background spectrum was collected, and then 5 mbar of CO was adsorbed at this temperature for 30 min (fifth step). Following evacuation, 15 min of desorption time was allowed (sixth step), and the sample was heated up to 473 K (seventh step). IR spectra were recorded during the CO adsorption at 10 and 30 min (fifth step), following the evacuation at 300 K (sixth step), and then during the heating up (seventh step) at 373, 423, and 473 K.

Characterization by NH_3-TPD. NH_3-TPD was used to determine the concentration of acid sites on the samples. About 50 mg powdered samples were placed in a Netzsch STA 409 PG/PC microbalance. After activation in a nitrogen gas stream at 573 K for 30 min, ammonia adsorption was carried out at 353 K in a N_2 flow, using a mixture of 10 vol % NH_3 in N_2 and a total flow of 40 cm^3/min for 1 h. After flushing the sample with pure N_2 at 353 K for 1 h in order to remove physisorbed NH_3, the TPD was carried out in a N_2 flow with a heating rate of 10 K/min up to 973 K.

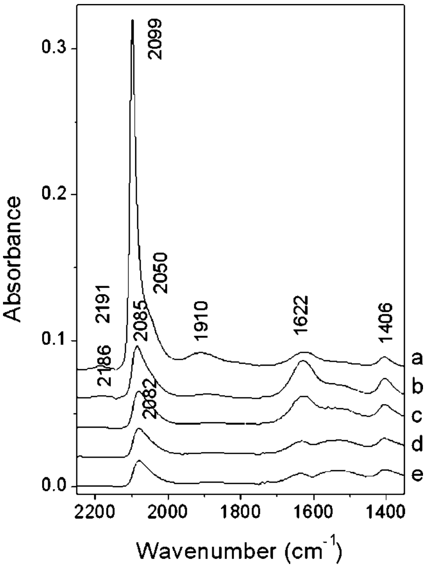

Figure 1. IR spectra of adsorbed CO on the reduced SBA20 catalyst as a function of the 5 mbar CO adsorption time (for 10 (a) and for 30 min (b)) and following evacuation at 300 K (c) and during annealing at 373 (d) and 423 K (e).

Results and Discussion

The IR spectra of CO adsorbed on the SBA20 catalyst are shown in Figure 1. All different characteristic ν_{CO} absorption bands observed in the literature[13,14] over silica (SiO_2)-supported nickel phosphide catalysts were identified in the infrared spectra (Table 1): CO terminally bonded to P (ν_{as} $P{=}C{=}O$) between 2191 and 2186 cm^{-1}, CO terminally bonded to cus (coordinatively unsaturated) $Ni^{\delta+}$ ($0 < \delta < 1$) sites ($Ni^{\delta+}{-}CO$) between 2099 and 2082 cm^{-1}, nickel tetracarbonyl formation ($Ni(CO)_4$) around 2050 cm^{-1}, and CO adsorbed on $Ni^{\delta+}$ bridge sites ($Ni^{\delta+}_2 > CO$) at 1910 cm^{-1}. Additional bands assigned to surface carbonates (CO_3^{2-}) were also observed in the 1600−1400 cm^{-1} region (Figure 1). Compared to the 10 min CO adsorption time (Figure 1a), following 30 min of equilibration (Figure 1b), the formation of $Ni(CO)_4$ and adsorption of CO on Ni bridge sites are strongly suppressed, and the relative intensity of the $Ni^{\delta+}{-}CO$ band decreases, while the intensity of carbonate bands increases. Following evacuation (Figure 1c) and heating up to 423 K (Figure 1d−e), the ν_{as} $P{=}C{=}O$ band disappears, the intensity of carbonate bands gradually decreases, but the $Ni^{\delta+}{-}CO$ band hardly changes, indicating that CO is adsorbed most strongly on the cus $Ni^{\delta+}$ sites. The spectrum of the catalytically very active[8] SBA20 catalyst after 10 min of equilibration time at room temperature (Figure 1a) was the most

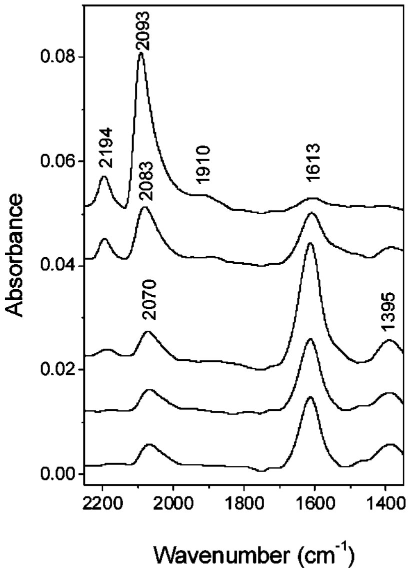

Figure 2. IR spectra of adsorbed CO on the reduced SBA_E catalyst as a function of the 5 mbar CO adsorption time (for 10 (a) and for 30 min (b)) and following evacuation at 300 K (c) and during annealing at 373 (d) and 423 K (e).

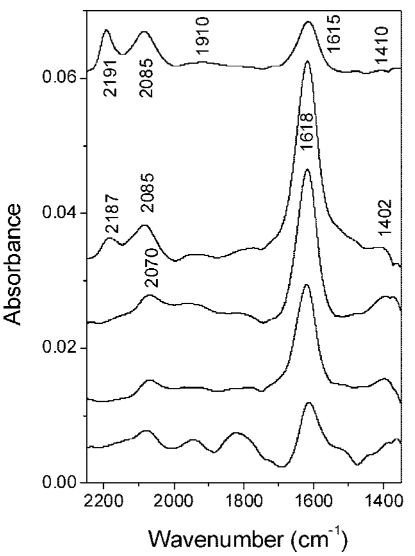

Figure 3. IR spectra of adsorbed CO on the reduced SBA_H catalyst as a function of the 5 mbar CO adsorption time (for 10 (a) and for 30 min (b)) and following evacuation at 300 K (c) and during annealing at 373 (d) and 423 K (e).

similar to the spectra of silica-supported samples published in the literature,[13,14] indicating the formation of analogue surface species.

We have studied the effect of excess phosphorus on the adsorption of CO on SBA20 catalysts. It is well-known that CO does not interact with Ni atoms blocked by phosphorus.[14,16] Comparing the spectra of stoichiometric P-containing SBA20 samples (Figure 1) with the spectra of excess- and high excess-P-containing SBA_E (Figure 2) and SBA_H (Figure 3) catalysts, the relative intensity of $Ni^{\delta+}-CO$ signals compared to the intensity of the ν_{as} P=C=O bands gradually decreases, in agreement with the decreasing reduced nickel surface site concentration of the SBA_H compared to that of SBA20 samples.[8] In parallel, the frequency of linear $Ni^{\delta+}-CO$ stretchings gradually shifts to lower wavenumbers with increasing P content, indicating bond strength weakening, but the frequency of the ν_{as} P=C=O signals hardly changes (Table 1). The frequency shift is due to the withdrawing of electron density from Ni atoms by P atoms, resulting a wide range of $Ni^{\delta+}$ ($0 < \delta < 1$) surface species.[13] Phosphorus hinders CO adsorption on $Ni^{\delta+}$ bridge sites and also hinders $Ni(CO)_4$ formation.[13] Following a longer (30 min) CO equilibration time and evacuation, the relative intensity of carbonate bands compared to the intensity of CO stretching signals increases, indicating the oxidation of surface species. As more oxidized phosphate surface species are also present,[7,8] these results suggest that CO is bonded to the reduced phosphides but not to oxidized phosphates. Normal coordinate analysis carried out for H−P=C=O yielded an antisymmetric stretching frequency for the P=C=O group of 2164−2195 cm^{-1},[17] in good agreement with the range of 2185−2194 cm^{-1} that we observed for reduced surface-bonded P=C=O species on these catalysts (Table 1).

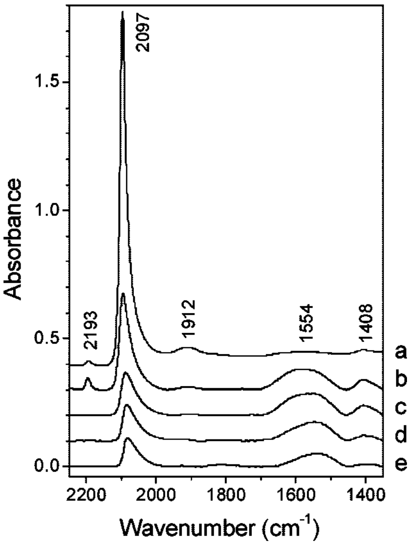

Figure 4. IR spectra of adsorbed CO on the reduced KIT20 catalyst as a function of the 5 mbar CO adsorption time (for 10 (a) and for 30 min (b)) and following evacuation at 300 K (c) and during annealing at 373 (d) and 423 K (e).

The effect of catalyst support has also been studied in this work. The only practical difference between the SBA-15 and KIT-6 supports is the two-dimensional structure of the former and the three-dimensional structure of the latter. In accordance with this minor difference, the infrared spectra of adsorbed CO on the KIT20 catalyst (Figure 4) were very similar to the spectra of the SBA20 (Figure 1) catalyst. The $Ni^{\delta+}-CO$ stretching frequencies of both catalysts shift with a remarkable 15 (or 5) cm^{-1} value to higher wavenumbers compared to the absorbance of the reduced (or sulfided) Ni_2P/SiO_2 catalyst (Table 1). This shift is attributed to the reduced P atoms, which withdraw electron density from the Ni atoms, weakening the interaction between CO and Ni and giving the Ni atoms a partial positive charge and the P atoms a partial negative charge.[13] The frequency of the ν_{as} P=C=O band does not change during equilibration of adsorbed CO, but it is clearly seen in the spectra (Figure 4), that all other bands gradually shift to lower wavenumbers during the equilibration−evacuation−annealing cycle (Table 1). This gradual bond strength weakening is in accordance with the expectations: different $Ni^{\delta+}$ ($0 < \delta < 1$) surface species lead to different bond strengths, but the reduced phosphide species seems to form P=C=O bonds with a more homogeneous strength.

The nickel phosphide active phase content (the loading) was also varied on both supports. The C−O stretching absorption in the 1800−2200 cm^{-1} frequency region could not be observed

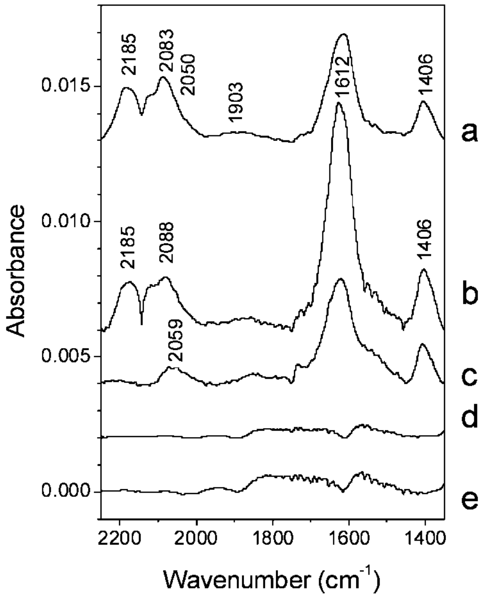

Figure 5. IR spectra of adsorbed CO on the reduced SBA10 catalyst as a function of the 5 mbar CO adsorption time (for 10 (a) and for 30 min (b)) and following evacuation at 300 K (c) and during annealing at 373 (d) and 423 K (e).

TABLE 2: Average Temperatures (K) of Mass Loss Steps (wt %) during NH_3-TPD on Reduced Catalyst Samples

	signal I		signal II	
catalyst	$T_{average}$ (K)	mass loss (wt %)	$T_{average}$ (K)	mass loss (wt %)
SBA_H	416	0.74	652	1.39
SBA_E	410	0.89	650	0.65
SBA20	409	0.63	651	0.35
SBA30	411	0.61	647	0.83
SBA10	406	0.52	651	0.59
KIT20	410	0.79	646	0.44
KIT30	412	0.46	650	0.40

in the spectra of the catalytically most active SBA30[18] and KIT30[19] catalysts due to their high (30 wt %) nickel phosphide loadings and their blackness, which resulted in nontransparency for the infrared radiation. The infrared spectra of adsorbed CO on the SBA10 catalyst with 10 wt % loading are shown in Figure 5. Due to the very low absorbance of adsorbed CO, the bands of CO in the gas phase are also seen in the spectra. Some ν_{as} P=C=O (at 2185 cm^{-1}) and $Ni^{\delta+}$−CO (at 2083−2088 cm^{-1}) bands are superposed to the underlying doublet-like band envelope of gaseous CO, when 5 mbar of CO is adsorbed (Table 1). The band intensity and shift changes during equilibration and evacuation are similar to those of the SBA20 catalyst, but during annealing, practically all bands disappear (Figure 5), indicating the presence of few surface active species due to low loading of SBA10 compared to that of the SBA20 sample.

The nature of surface acidity can be revealed by NH_3-TPD. The strength of acid sites is related to the corresponding desorption temperature. Generally, the acid sites are classified into weak (473 K), medium (473−623 K), and strong (623 K) acid sites.[20] Two mass loss steps were distinguished in the thermogravimetric (TG) and differential thermogravimetric (DTG) curves of the catalysts. The low-temperature mass loss step at 406−416 K (Table 2) can be attributed to the release of ammonia from the weak acidic sites, which arise from surface hydroxyl group attached to Si.[20] The high-temperature step at 646−652 K belongs to the strong acidic sites. The NH_3-TPD profile for the pure SBA-15 material shows only one desorption peak centered around 368 K.[21] The SBA_H catalyst released the highest amount of ammonia at the high-temperature step (Table 2), indicating a high concentration of strong acidity, which can be attributed to the Brönsted acidic surface phosphate species. As the hydrotreating activity of the SBA_H catalyst is relatively low within these catalysts,[8,18] it is suggested that high strong Brönsted acidity is not advantageous for hydrotreating reactions.

Conclusions

The same CO adsorbed species have been identified on the surface of SBA-15- and KIT-6-supported nickel phosphide hydrotreating catalysts as on the surface of Ni_2P/SiO_2 catalysts published in the literature.[13,14] The frequency of the most intense $Ni^{\delta+}$−CO vibration shifted to higher wavenumbers in the spectra of SBA20 and KIT20 compared to this vibration of silica-supported nickel phosphide catalysts, indicating a modified Ni−P charge distribution. The surface-active species are presumably similar in these catalysts.

During the CO equilibration−evacuation−annealing cycle, all CO stretching bands shifted to lower wavenumbers, indicating a gradually decreasing bond strength. The lowest degree of shift occurred at the ν_{as} P=C=O frequencies, indicating a relatively homogeneous phosphide P=C=O bond strength. The $Ni^{\delta+}$−CO bond together with the gradually forming carbonate species proved to be the most stable bonds.

The strong acidity of high excess-phosphorus-containing SBA_H catalysts can be attributed to the surface phosphate or even phosphoric acid species, in agreement with the NMR results published elsewhere.[7,8]

The relatively high catalytic activity of SBA20[7,8] and KIT20 samples can be connected to their weak acidities and to the small relative intensity of the ν_{as} P=C=O bands in their spectra, consequently with the lack of surface phosphoric acid.

The modified Ni−P charge distribution presumably plays a role in the higher hydrotreating activity of SBA-15- and KIT-6 supported nickel phosphide catalysts compared to the activity of Ni_2P/SiO_2 catalysts.

Acknowledgment. This work was supported by The Hungarian Austrian Intergovernmental S & T Cooperation Programme (TÉT Grant No. A-15/2005). Special thanks are due to Prof. R. Ryoo and Dr. H.S. Kim (KAIST, Korea) for preparation of part of the catalysts.

References and Notes

(1) Topsøe, H.; Clausen, B. S.; Massoth, F. E. *Hydrotreating Catalysis*; Springer: Berlin, Germany, 1996.
(2) Oyama, S. T. *J. Catal.* **2003**, *216*, 343.
(3) Shu, Y.; Oyama, S. T. *Carbon* **2005**, *43*, 1517.
(4) Shu, Y.; Oyama, S. T. *Chem. Commun.* **2005**, 1143.
(5) Wang, A.; Ruan, Y.; Teng, Y.; Li, X.; Lu, M.; Ren, J.; Wang, Y.; Hu, Y. *J. Catal.* **2005**, *229*, 314.
(6) Nava, R.; Morales, J.; Alonso, G.; Ornelas, C.; Pawelec, B.; Fierro, J. L. G. *Appl. Catal., A* **2007**, *32*, 1.
(7) Korányi, T. I.; Vít, Z.; Nagy, B. J. *Catal. Today* **2008**, *130*, 80.
(8) Korányi, T. I.; Vít, Z.; Poduval, D. G.; Ryoo, R.; Kim, H. S.; Hensen, E. J. M. *J. Catal.* **2008**, *253*, 119.
(9) Choi, M.; Heo, W.; Kleitz, F.; Ryoo, R. *Chem. Commun.* **2003**, 1340.
(10) Knözinger, H. *Adv. Catal.* **1976**, *25*, 184.
(11) Ballinger, T. H.; Yates, J. T., Jr *Langmuir* **1991**, *7*, 3041.
(12) Korányi, T. I.; Mihály, J.; Pfeifer, É.; Németh, Cs.; Yuzhakova, T.; Mink, J. *J. Phys. Chem. A* **2006**, *110*, 1817.
(13) Layman, K. A.; Bussell, M. E. *J. Phys. Chem. B* **2004**, *108*, 10930.
(14) Sun, F.; Wu, W.; Wu, Z.; Guo, J.; Wei, Z.; Yang, Y.; Jiang, Z.; Tian, F.; Li, C. *J. Catal.* **2004**, *228*, 298.

(15) Kim, T. W.; Kleitz, F.; Paul, B.; Ryoo, R. *J. Am. Chem. Soc.* **2005**, *127*, 7601.

(16) Oyama, S. T.; Wang, X.; Lee, Y.-K.; Chun, W.-J. *J. Catal.* **2004**, *221*, 263.

(17) Nguyen, M. T.; Hegarty, A. F.; McGinn, M. A.; Ruelle, P. *J. Chem. Soc., Perkin Trans. 2* **1985**, 1991.

(18) Korányi, T. I.; Ryoo, R.; Kim, H. S.; Hensen, E. J. M.; Pfeifer, É.; Szegedi, Á.; Mihályi, M. R. *Extended Abstract*, 14th International Congress on Catalysis, Seoul, Korea; 2008.

(19) Korányi, T. I.; Ryoo, R.; Kim, H. S.; Hensen, E. J. M.; Pfeifer, É.; Szegedi, Á.; Mihályi, M. R.; Nagy, B. J. *Abstract*, 6th International Mesostructured Materials Symposium, Namur, Belgium; 2008.

(20) Sundaramurthy, V.; Eswaramoorthi, I.; Dalai, A. K.; Adjaye, J. *Microporous Mesoporous Mater.* **2008**, *111*, 560.

(21) Chena, Y.; Han, J.; Zhang, H. *Appl. Surf. Sci.* **2007**, *253*, 9400.

JP711935N